

# $p$ -wave phase shift and scattering length of ${}^6\text{Li}$

S. Gautam\* and D. Angom†  
Physical Research Laboratory  
Navarangpura, Ahmedabad - 380 009

We have calculated the  $p$ -wave phase shifts and scattering length of  ${}^6\text{Li}$ . For this we solve the  $p$  partial wave Schrödinger equation and analyze the validity of adopting the semiclassical solution to evaluate the constant factors in the solution. Unlike in the  $s$  wave case, the semiclassical solution does not provide unique value of the constants. We suggest an approximate analytic solution, which provides reliable results in special cases. Further more, we also use the variable phase method to evaluate the phase shifts. The  $p$ -wave scattering lengths of  ${}^{132}\text{Cs}$  and  ${}^{134}\text{Cs}$  are calculated to validate the schemes followed. Based on our calculations, the value of the  $p$  wave scattering length of  ${}^6\text{Li}$  is  $-45a_o$ .

PACS numbers: 34.50.-s, 34.10.+x

## I. INTRODUCTION

For bosonic isotopes of atoms, one parameter which describes the low energy scattering properties is  $a_0$ , the  $s$ -wave scattering length. It arises from the  $s$ -wave phase shift  $\eta_0$ . The corresponding interaction potential is a crucial parameter in Bose Einstein condensates of dilute ultracold atomic gases. The fermionic counterpart is the interaction potential arising from the  $p$ -wave scattering. Calculations of which is important as experiments on fermionic isotopes have made impressive strides since the first experimental observation of degenerate fermions [1]. Superfluidity in two species fermionic mixture of  ${}^6\text{Li}$ , which was first predicted theoretically [2], has been observed without any ambiguity [3, 4, 5]. Following which, intense experimental and theoretical investigations continues on the phase diagram of the spin polarized two component  ${}^6\text{Li}$  mixture. Among the most recent developments are the theoretical investigation of the phase diagram at finite temperature [6] and the experimental investigation of the same at unitarity [7]. Further, the recent achievement of cooling the  ${}^6\text{Li}$ - ${}^{40}\text{K}$  fermionic mixture to degeneracy [8] takes us closer to observing exotic phases predicted for spin polarized heteronuclear fermionic mixtures [9]. Some of the predicted phases are fragile and crucially dependent on the difference of the chemical potentials. For such cases, the change in chemical potential induced by the  $p$ -wave scattering is likely to be an important parameter. The pseudopotentials arising from the higher partial waves, discussed in recent works [10, 11], can be used to incorporate the effects of  $p$ -wave scattering in fermionic isotopes.

In this paper we describe the calculation of the  $p$ -wave scattering length of  ${}^6\text{Li}$ . As suggested in an earlier work on  $s$ -wave scattering [12], the WKB method is used to determine the constant parameters of the partial wave solutions of the Schrödinger equation. However, unlike

in the  $s$ -wave scattering, the parameters in the  $p$ -wave calculations has radial dependence. This is an outcome of including the centrifugal potential in the effective interatomic potential. To circumvent this, an analytic expression, which provide an estimate of the  $p$ -wave phase shift is suggested. This method is valid when the dispersion constant  $C_6$  is large. We also calculate the phase shift using the variable phase method. To test and validate the numerical schemes adopted, the  $s$ -wave phase shift of  ${}^{133}\text{Cs}$  and  $p$ -wave scattering length of  ${}^{132}\text{Cs}$  and  ${}^{134}\text{Cs}$  are calculated.

For completeness in Section.I of the paper, we provide an outline of solving the  $p$  partial wave Schrödinger equation in different radial regions. The Section.II discusses the calculation of the scattering length using the WKB method to determine the constants in the partial wave solutions. Then a brief description of the variable phase method is provided in Section.III, this is followed with results and conclusions. All the equations and results in this paper are in atomic units, in which  $\hbar = m_e = e = 1$ .

## II. $p$ -WAVE PHASE SHIFT

The radial part of the Schrodinger wave equation for collisions between two atoms with  $V(R)$  as the interatomic potential is

$$\frac{d^2\chi}{dR^2} + \left[ k^2 - U(R) - \frac{l(l+1)}{R^2} \right] \chi = 0, \quad (1)$$

Here  $U(R) = 2mV(R)$ ,  $k$  is the relative momentum of the two atoms,  $l$  is the angular momentum quantum number and  $\chi(R)$  is the radial wave-function. This equation can be used to calculate scattering phase shifts ( $\eta_l$ ) which each component angular momentum suffers due to the interaction with the scattering center. At low energies we can calculate approximate solution of Eq. (1) in three difference radial ranges. These are the  $kR \ll 1$ ,  $kR < 1$  and  $kR \approx 1$  regions.

\*Electronic address: sandeep@prl.res.in

†Electronic address: angom@prl.res.in

### A. $kR \ll 1$ region

In this region, we can neglect the  $k^2$  term

$$\frac{d^2\chi}{dR^2} + \left[ -U(R) - \frac{l(l+1)}{R^2} \right] \chi = 0, \quad (2)$$

and hence, the solution is independent of  $k$ . At large distances from the scattering center, van der Waal's potential  $U(R) = -2m\alpha/(R^6) = -\gamma^2/R^6$  is the dominant inter-atomic interaction. Here,  $\alpha$  is the van der Waal's coefficient. For low energy collisions  $k \rightarrow 0$ , the interatomic potential approaches the asymptotic form within the  $kR \ll 1$  region. Then,

$$\frac{d^2\chi}{dR^2} + \left[ \frac{\gamma^2}{R^6} - \frac{l(l+1)}{R^2} \right] \chi = 0. \quad (3)$$

Substituting  $\chi(R) = \xi(R)\sqrt{R}$  and  $R = \sqrt{\gamma/2x}$ , we obtain the Bessel differential equation of order  $(2l+1)/4$

$$\frac{d^2\xi}{dx^2} + \left[ 1 - \frac{(2l+1)^2}{16x^2} \right] \frac{d\xi}{dx} = 0.$$

The general solution of Eq.(3) is

$$\chi(R) = \sqrt{R} \left[ AJ_{(2l+1)/4} \left( \frac{\gamma}{2R^2} \right) + BJ_{-(2l+1)/4} \left( \frac{\gamma}{2R^2} \right) \right].$$

Considering the  $p(l=1)$  partial wave

$$\chi(R) = \sqrt{R} \left[ AJ_{3/4} \left( \frac{\gamma}{2R^2} \right) + BJ_{-3/4} \left( \frac{\gamma}{2R^2} \right) \right]. \quad (4)$$

In the limit  $R \rightarrow \infty$  or  $x \rightarrow 0$ , where  $kR < 1$ , the leading terms in the series expansion of  $J_{3/4}(x)$  and  $J_{-3/4}(x)$  are dominant and the remaining terms are negligible

$$\chi(R) = B \frac{(\gamma/2)^{-3/4} R^2}{2^{-3/4} \Gamma(1/4)} + A \frac{(\gamma/2)^{3/4}}{2^{3/4} \Gamma(7/4) R}, \quad (5)$$

where  $\Gamma(\dots)$  are the gamma functions.

### B. $kR < 1$ region

In this region, we can neglect the interatomic interaction potential  $U(R)$ , if it approaches zero faster than  $1/R^2$ . In addition, as in the  $kR \ll 1$  region, the  $k^2$  term can be neglected

$$\frac{d^2\chi}{dR^2} - \frac{l(l+1)}{R^2} \chi = 0. \quad (6)$$

The most general solution of this equation is

$$\chi(R) = aR^{l+1} + bR^{-l}. \quad (7)$$

For  $l=1$ , comparing the solutions in Eq. (5) and Eq. (7)

$$a = B \frac{(\gamma/2)^{-3/4}}{2^{-3/4} \Gamma(1/4)} \quad \text{and} \quad b = A \frac{(\gamma/2)^{3/4}}{2^{3/4} \Gamma(7/4)}. \quad (8)$$

The comparison is possible as  $\chi$  in the  $R \rightarrow \infty$  of Eq.(4) has the same form as the solution in the  $kR < 1$  region.

### C. $kR \approx 1$ region

Increasing  $R$  further, we enter the  $kR \approx 1$  region. In this region, we can neglect  $U(R)$  in comparison to the other terms in Eq. (1), then

$$\frac{d^2\chi}{dR^2} + \left[ k^2 - \frac{l(l+1)}{R^2} \right] \chi = 0. \quad (9)$$

This is the Schrödinger equation in the asymptotic region and the solution is a plane wave of wave number  $k$ . However, the interatomic potential introduces a phase shift  $(\eta_l)$ [15] to the plane wave

$$\chi(R) = CR^{1/2} [J_{l+1/2}(kR) + (-1)^l \tan(\eta_l) J_{-l-1/2}(kR)].$$

Expanding the Bessel's functions  $J_{l+1/2}(kR)$  and  $J_{-l-1/2}(kR)$ , the solution when  $kR < 1$  is

$$\chi(R) = \left( \frac{2k}{\pi} \right)^{1/2} C \left[ R^{l+1} \frac{(2k)^l \Gamma(l+1)}{\Gamma(2l+2)} + R^{-l} \tan \eta_l \frac{(2k)^{-l-1} 2\Gamma(2l+1)}{\Gamma(l+1)} \right]. \quad (10)$$

Equating the solutions in Eq. (7) and (10)

$$\tan \eta_l = \frac{b 2^{2l} (\Gamma(l+1))^2}{a \Gamma(2l+1) \Gamma(2l+2)} k^{2l+1}. \quad (11)$$

Since  $b/a$  is independent of  $k$ ,  $\tan \eta_l$  varies as  $k^{2l+1}$ . It should also be mentioned that, though the entire radial range is divided into three domains, the solutions are in the asymptotic region. This defines the phase shift  $\eta_l$  in terms of the  $b/a$  and it is strictly applicable for  $k \rightarrow 0$ . For the  $p$ -partial wave

$$\tan \eta_1 = \frac{b}{a} \frac{4}{\Gamma(3) \Gamma(4)} k^3. \quad (12)$$

In the above expression, to calculate  $\eta_1$ , the ratio  $b/a$  should be determined. From the Eq.(8), the phase shift can also be defined in terms of  $A/B$  as

$$\tan \eta_1 = \frac{1}{24} \frac{A}{B} \frac{\gamma^{3/2} \Gamma(1/4)}{\Gamma(7/4)} k^3. \quad (13)$$

Here the actual values of  $\Gamma(3)$  and  $\Gamma(4)$  are used. Now onwards this definition of  $\eta_1$  is used. As the phase shift  $\eta_1$  has functional dependence on  $\tan^{-1}$ , which has a domain of  $[-\infty, \infty]$ , its accuracy is sensitive to the value of  $A/B$ .

## III. SCATTERING LENGTH CALCULATION

As mentioned earlier, the expression of  $\eta_1$  in Eq.(13) is in the asymptotic domain of the interatomic potential and require evaluation of  $A/B$ . The solution of the Schrödinger equation Eq.(1) in the asymptotic region,

given by Eq.(4) and parametrized in terms of  $A$  and  $B$ , is the outer solution. To determine  $A/B$ , the Eq.(1) should be solved within the inner part of the interatomic potential: inner wall and well. This can be evaluated using the WKB method [12]. Matching the solutions, outer and inner, at a point we can evaluate  $A/B$ . The matching point should be in the region where the asymptotic form of the interatomic potential begins to dominate but the WKB solution is still valid.

### A. WKB solution

For partial waves other than  $s$ , the centrifugal potential is nonzero. Combining the the interatomic potential and centrifugal term, the effective interatomic potential

$$U_{\text{eff}}(R) = U(R) + l(l+1)/R^2. \quad (14)$$

Then the local momentum of the scattered atom  $p(R) = \sqrt{-U_{\text{eff}}(R)}$ , and the de Broglie wavelength  $\lambda(R) = 2\pi/\sqrt{-U_{\text{eff}}(R)}$ . The WKB approximation is applicable when

$$\left| \frac{d\lambda}{dR} \right| \ll 2\pi \quad \text{or} \quad \frac{m|F|}{p^3} \ll 1. \quad (15)$$

In above relation  $F = -dU_{\text{eff}}/(2mdR)$  is the net force acting on the atom. At large distances, when the interatomic potential approaches the asymptotic form, the above inequality for  $l = 1$  is

$$\left[ \frac{3\gamma^2}{R^4} - 2 \right] \ll \left[ \frac{\gamma^2}{R^4} - 2 \right]^{3/2}. \quad (16)$$

This inequality is in general valid up to large radial distances. As an example Fig.1 shows that for Cs the inequality is satisfied up to  $\approx 30$ . Then the WKB solution at  $R$  which satisfies the inequality and larger then the classical turning point  $R_o$  is

$$\chi(R) = \frac{c}{\sqrt{p}} \cos \left( \int_{R_o}^R p dR - \frac{\pi}{4} \right) \quad (17)$$

and the logarithmic derivative is

$$\begin{aligned} \zeta(R) &= \frac{\chi'(R)}{\chi(R)} \\ &= -p(R) \tan \left( \int_{R_o}^R p dR - \frac{\pi}{4} \right) - \frac{1}{2p} \frac{dp}{dR}. \end{aligned} \quad (18)$$

An analytic expression of  $\zeta(R)$  for  $l = 1$  is obtained if only the van der Waal's potential is considered

$$\begin{aligned} \zeta(R) &= -\frac{\sqrt{\gamma^2 - 2R^4}}{R^3} \tan \left[ \frac{\sqrt{\gamma^2 - 2R_o^4}}{2R_o^2} - \frac{\sqrt{\gamma^2 - 2R^4}}{2R^2} \right] \\ &\quad - \frac{1}{\sqrt{2}} \left( \sin^{-1} \frac{\sqrt{2}R^2}{\gamma} - \sin^{-1} \frac{\sqrt{2}R_o^2}{\gamma} \right) - \frac{\pi}{4} \\ &\quad - \left[ \frac{2R^4 - 3\gamma^2}{2R(\gamma^2 - 2R^4)} \right]. \end{aligned} \quad (19)$$

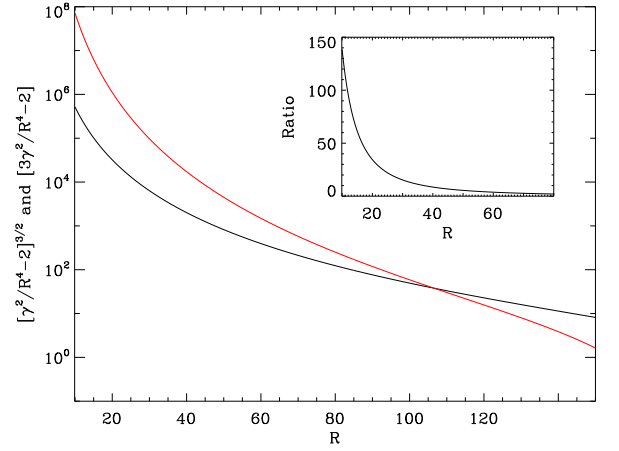


FIG. 1: Terms in the relation  $[3\gamma^2/R^4 - 2] \ll [\gamma^2/R^4 - 2]^{3/2}$  which defines the validity of the WKB solution are plotted for Cesium. The red and black curves correspond to  $[\gamma^2/R^4 - 2]^{3/2}$  and  $[3\gamma^2/R^4 - 2]$  respectively. Inset shows the ratio of the two terms.

This approximation neglects the well and inner wall part of the interatomic potential. It is appropriate for model potentials comprising of the van der Waal's and hard core potential. The above expression is reduced to that of  $s$  case when  $l = 0$ , which is used implicitly in ref. [12].

From the inequality (16), it is evident that when  $\gamma$  is sufficiently large, WKB solution is valid up to radial distances where the asymptotic form of the potential begins to dominate. Choose a point  $R^*$  in this region, such that the 2 in the inequality can be neglected. Then the inequality is modified to

$$R^* \ll (\gamma/3)^{1/2}. \quad (20)$$

At this point, as the interatomic potential has the asymptotic form, Eq. (4) is a solution of the Schrödinger equation Eq.(1). This is discussed in Section.II A.

### B. Matching $\chi'(R)/\chi(R)$

From the definition, at  $R^*$  and around it  $x = \gamma/(2R^{*2}) \gg 1$ . Where  $x$  is the variable first used in Section II A. We can then use the asymptotic expression of the Bessel's function

$$\lim_{x \rightarrow \infty} J_n(x) \simeq \sqrt{\frac{2}{\pi x}} \cos \left[ x - \left( n + \frac{1}{2} \right) \right],$$

and the solution in Eq. (4) is

$$\begin{aligned} \chi(R) &= \frac{2R^{3/2}}{\sqrt{\pi\gamma}} \left[ A \cos \left( \frac{\gamma}{2R^2} - \frac{5\pi}{8} \right) + \right. \\ &\quad \left. B \cos \left( \frac{\gamma}{2R^2} + \frac{\pi}{8} \right) \right]. \end{aligned} \quad (21)$$

This is the inner limit of the asymptotic solution. Whereas the solution in Eq.(5), in the  $x \rightarrow 0$ , is the outer

limit of the asymptotic solution. To determine  $A/B$  we match the logarithmic derivatives of the analytical solution in Eq. (21) and WKB solution in Eq. (17). The ratio is

$$\frac{A}{B} = \frac{\sqrt{2m\alpha} \sin \phi_2 - R^{*2}[R^*\zeta(R^*) - 3/2] \cos \phi_2}{R^{*2}[R^*\zeta(R^*) - 3/2] \cos \phi_1 - \sqrt{2m\alpha} \sin \phi_1}, \quad (22)$$

here  $\phi_1 = \gamma/(2R^{*2} - 5\pi/8)$ ,  $\phi_2 = \gamma/2R^{*2} + \pi/8$ . It is evident from the above expression that  $A/B$  depends on the choice of the matching point  $R^*$ . This implies that  $\eta_1$  and hence the scattering length, to be defined later, depend on  $R^*$ . This radial dependence arises from the centrifugal part in the expression of the effective potential  $U_{\text{eff}}(R)$ . Neglecting the terms arising from the centrifugal potential in the expression of  $\zeta(R)$ , logarithmic derivative of the WKB solution is

$$\zeta(R) = -\frac{\gamma}{R^3} \tan \left( \frac{\gamma}{2} \left( \frac{R^2 - R_o^2}{R^2 R_o^2} \right) - \frac{\pi}{4} \right) + \frac{3}{2R}. \quad (23)$$

For the obvious reason, large value of  $R/\gamma$ , this expression is not valid at very large values of  $R$ . Assuming that the maximum radial distance at which the above expression is valid, the interatomic potential has the asymptotic form. If  $A/B$  is calculated using Eq. (23) as the WKB solution, it is then independent of the choice of matching point

$$\frac{A}{B} = -\frac{\sin(\phi - \frac{\pi}{8})}{\sin(\phi - \frac{7\pi}{8})}, \quad (24)$$

where  $\phi = \gamma/(2R_o^2)$ . This is however a crude estimate as the outer solution includes the effect of centrifugal term but the inner solution, the WKB solution, does not. Still, it is a useful estimate, as it is an analytic expression and not difficult to evaluate.

### C. $p$ -wave scattering length

For any arbitrary potential which vary as  $R^{-n}$ , the scattering length ( $a_l$ ) and phase shift ( $\eta_l$ ) are related as [15]

$$\lim_{k \rightarrow 0} k^{2l+1} \cot \eta_l = \frac{-1}{a_l^{2l+1}}. \quad (25)$$

This relation is valid provided  $l < (n-3)/2$  and is applicable for  $p$  partial wave when  $n = 6$  or higher. From Eq. (13) and (25) scattering length of the  $p$  partial wave is

$$a_1^3 = -\frac{1}{24} \frac{A}{B} \frac{\gamma^{3/2} \Gamma(1/4)}{\Gamma(7/4)}. \quad (26)$$

Using the value of  $A/B$  in Eq. (22), the  $p$ -wave scattering length  $a_1$  can be evaluated. A rough estimate of  $a_1$  is to use the analytical expression in Eq. (24). The quantity  $a_1^3$  is referred to as the  $p$  wave scattering volume. It is an important parameter in the three-body recombination of identical, spin polarized fermions in low temperatures [16].

## IV. VARIABLE PHASE METHOD

Another approach to calculate  $a_1$  is to evaluate  $\eta_1$  from the phase function equation, which is referred to as the variable phase method [13]. The method is applicable when the interatomic potential satisfies two conditions. First condition is, the interatomic potential should be less singular at origin than the centrifugal part, that is

$$\lim_{R \rightarrow 0} [R^2 U(R)] = 0. \quad (27)$$

This implies that, near the origin  $U(R) \rightarrow U_0 R^m$  as  $R \rightarrow 0$ , with  $m > -2$ , where  $U_0$  is a constant. The interatomic potential satisfies this condition since at smaller radial distances, it approaches the inner wall and is repulsive.

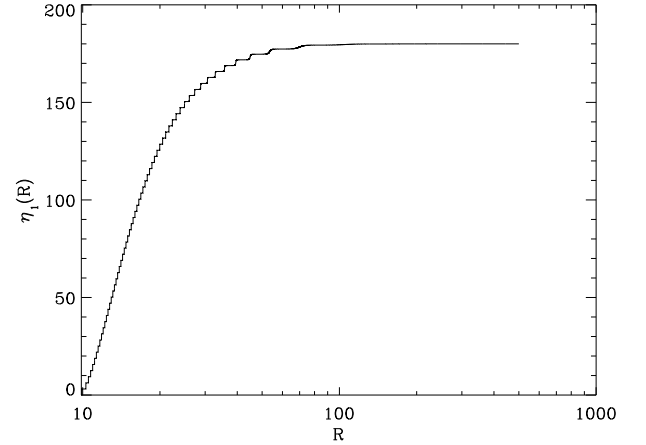


FIG. 2: The phase function  $\eta_1(R)$  for  $^{134}\text{Cs}$  at  $k = 0.05$  in atomic units. The radial distance is in log scale and the plot shows  $\eta_1(R)$  up to  $R = 500a_0$ , where the phase function converges to an accuracy of  $10^{-6}$ .

The second condition is, the interatomic potential should decrease faster than the Coulomb potential or inverse of  $R$ . In the variable phase method, the phase shift  $\eta_l$  is a solution of the nonlinear differential equation [13]

$$\eta_l'(R) = -k^{-1} U(R) [\cos \eta_l(R) j_l(kR) - \sin \eta_l(R) n_l(kR)]^2, \quad (28)$$

where  $j_l(kR)$  and  $n_l(kR)$  are the spherical Bessel and Neumann functions respectively. The above equation can be used to evaluate the phase function  $\eta_l(R)$ , which defines the total phase shift upto  $R$ . Then the phase shift is the limiting value

$$\eta_l = \lim_{R \rightarrow \infty} \eta_l(R). \quad (29)$$

To calculate  $\eta_l$ , the phase function  $\eta_l(R)$  is evaluated upto a cut off point at which  $\eta_l(R)$  saturates. The physical implication of the cut off point is, it is the radial distance beyond which the inter atomic potential can be considered zero. To illustrate the radial dependence and saturation Fig. 2 shows  $\eta_1(R)$  for  $k = 0.05$  of  $^{134}\text{Cs}$ . The figure shows that, for the chosen parameters, saturation

occurs at  $\approx 500$ . The phase shift  $\eta_l$ , as it is evident from Eq. (28), depends on the relative momentum of the colliding atoms  $k$ . To remove the  $\text{mod}(\pi)$  ambiguity, the phase shift is normalized such that it approaches zero as  $k \rightarrow \infty$ , that is

$$\lim_{k \rightarrow \infty} \eta_l = 0. \quad (30)$$

In addition to above condition  $\eta_l$  is considered to be regular function of  $k$ . The Eq.(28) is numerically integrated from the classical turning point, where the inner wall starts, to the cut off point. The solution is the phase shift as defined in Eq.(29).

## V. RESULTS

To evaluate the phase shift and the scattering length, the interatomic potential should be known accurately. In this paper, we present the results of our calculations for cesium and lithium atoms. For which the interatomic potentials are known accurately and hyperfine interactions are less significant in the long range part of the potentials. The cesium interatomic potential is the one used in the work of Gribakin and Flambaum [12], which is based on ref [17]. The lithium interatomic potential is based on the work of Zemke and Stwalley [18]. The same authors and their collaborators have also calculated the interatomic potential of other alkali metals sodium [19] and potassium [20]. However, these are limited to radial distances where hyperfine interactions are not important.

Once the interatomic potential is known, the logarithmic derivative of the WKB solution  $\zeta(R)$ , given in Eq.(18) is evaluated numerically. To check the accuracy and validate the numerical schemes adopted, the numerically calculated  $\zeta(R)$  with only the van der Waal's potential is compared with the analytic expression in Eq.(19). The calculated  $\zeta(R)$  is then used in Eq.(22) to evaluate  $A/B$ . As discussed earlier, the calculated  $A/B$  has radial dependence and it is difficult to choose an appropriate matching point  $R^*$ . An estimate of  $R^*$  can however be obtained from the results of the variable phase calculations. Such a calculation provides a consistency check on the use of the WKB method. Despite the radial dependence, for the  $p$ -wave calculations the importance of using the WKB solution lies in Eq.(24), an analytic expression of  $A/B$ . From which, it is possible to calculate a rough estimate of the scattering length, which is in reasonable agreement with the numerical result for  $^{134}\text{Cs}$ . For  $^{132}\text{Cs}$  and  $^6\text{Li}$ , the two results are very different.

The phase shift  $\eta_1$  is also calculated from the phase function equation, for which the nonlinear differential equation Eq. (28) is numerically solved. In the present work, the Runge-Kutta-Fehlberg (RKF) method is used. With this method, it is possible to calculate phase shifts for small values of  $k$ , which is otherwise not possible with methods like fourth order Runge-Kutta. Calculations with the later method has large errors for small

values of  $k$ . For example, in the Cesium calculations with RK4 method, the calculated phase shifts are reliable up to  $k = 6.0 \times 10^{-3}$  and  $k = 1.1 \times 10^{-3}$  for  $p$  and  $s$  partial waves respectively. In comparison, with RKF method one can calculate phase shifts for still lower values of  $k$ . In the numerical calculations, to integrate the phase function differential equation, the classical turning point is chosen as the starting point. Then, zero is an appropriate initial value of  $\eta_1(R)$ . Using RKF we can calculate  $\eta_1(R)$  for different values of  $k$ . The  $\eta_1(R)$  is calculated till a point where it does not increase with further increase in  $R$ . This point is chosen as the cut off point where potential can be considered as zero and the corresponding value of the phase function is the required phase shift. To calculate the scattering length  $a_1$ , the phase shift  $\eta_1$  is evaluated for a range of  $k$  close to zero. This is essential as  $a_1$  depends on the nature of the  $\tan \eta_1$  close to  $k = 0$ . From the definition in Eq. (25),  $-\tan \eta_1/k^3$  converges to the scattering length for  $p$  partial wave as  $k \rightarrow 0$ . Alternatively,  $-\tan \eta_1/k^2$  is linear as  $k \rightarrow 0$  and the slope is the scattering length.

### A. Cesium

Consider the scattering of two Cesium atoms in the  $^3\Sigma_u$  state. The form of interaction potential is [17]

$$V(R) = \frac{1}{2}BR^\alpha \exp \beta R - \left( \frac{C_6}{R^6} + \frac{C_8}{R^8} + \frac{C_{10}}{R^{10}} \right) f_c(R). \quad (31)$$

where  $B = 0.0016$ ,  $\alpha = 5.53$  and  $\beta = 1.072$ . These are given in ref [12] and  $f_c(R)$  is the cut-off function and has the expression

$$f_c(R) = \Theta(R - R_c) + \Theta(R_c - R) \exp^{-(R_c/R-1)^2}, \quad (32)$$

where  $\Theta(\dots)$  is the step function which is equal to 1 or 0, depending on whether its argument is greater or less than zero. Here  $R_c$  is the cut off parameter. For comparison, the total interatomic potential  $V(R)$  and van der Waal's potential are shown in Fig.3. The ratio of the two are also shown as an inset plot. The figure shows that  $V(R)$  approaches the asymptotic form at around  $R = 24$ , where the ratio of the two is 0.8. Beyond  $R = 30$ , the two are indistinguishable. Using this potential, the phase shift and scattering lengths are calculated for the  $^{132}\text{Cs}$  and  $^{134}\text{Cs}$  fermionic isotopes. As test calculations, we evaluated the  $s$  wave phase shifts for the  $^{133}\text{Cs}$  isotope. It is to be mentioned that, the value of  $\gamma$  is 41240.1. However, in ref. [12] the value of  $\gamma$  is defined as 41200. Using the later, the results of the test calculations are in good agreement with that of ref. [12].

From Eq.(24), which provides a rough estimate, the value of  $a_1$  is 137a.u and  $-108$  a.u. for  $^{132}\text{Cs}$  and  $^{134}\text{Cs}$  respectively. The  $\eta_1$  calculated from the variable phase method, for different  $R_c$  for a range of  $k$  close to zero are shown in Fig.4. Our calculations show that, the value of  $\eta_1$  at higher values of  $k$  are sensitive to  $\gamma$ , the dependence



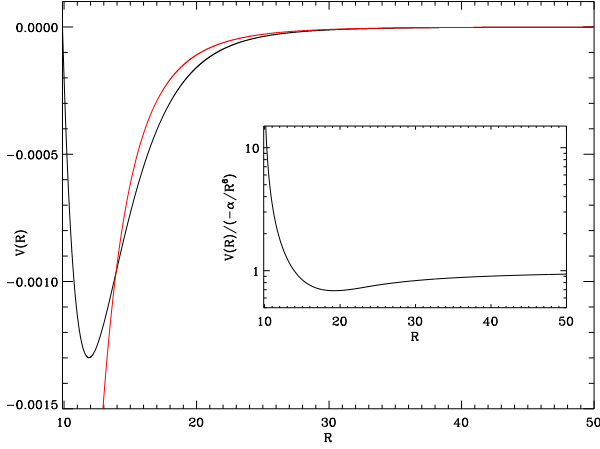


FIG. 3: The black and red curves are the plots of interatomic and the van der Waals potential respectively for Cesium. In the inset ratio of van der Waals term to the actual potential is plotted.

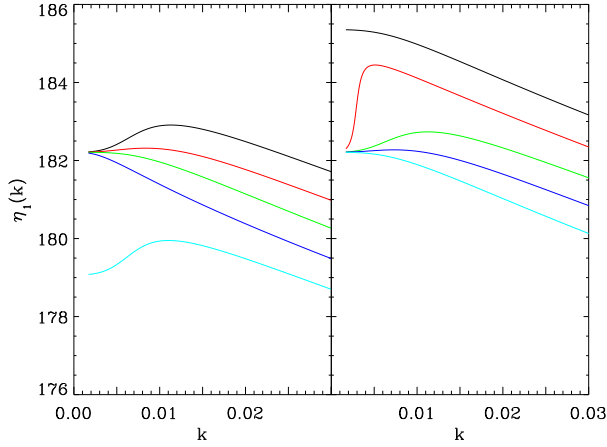


FIG. 4: The left and right panel of the figure are the phase shift  $\eta_1(k)$  of  $^{132}\text{Cs}$  and  $^{134}\text{Cs}$  isotopes respectively. Each panel show the plots of  $\eta_1(k)$  for different cut off radius  $R_c$  of the potential. The, black, red, green, blue and cyan correspond to  $R_c = 23.115, 23.140, 23.165, 23.190$  and  $23.215$  respectively.

is nonlinear as the equation of phase function is a non-linear differential equation. Consequently, small change in  $\gamma$  could result in significant change of  $\eta_1$ . The dependence  $\eta_1$  on  $\gamma$  for larger difference is evident from Fig.4, which shows  $\eta_1$  for  $^{132}\text{Cs}$  and  $^{134}\text{Cs}$ . The difference in the interatomic potential of the two isotopes is the mass, which manifests as unequal values of  $\gamma$ . There are two distinct differences in the results for the two isotopes: for the  $R_c = 23.215$  case  $\eta_1$  converges to 179.08 and 182.21 for  $^{132}\text{Cs}$  and  $^{134}\text{Cs}$  respectively; and for the  $R_c = 23.115$  case  $\eta_1$  converges to 182.22 and 185.35 respectively. The phase function in the neighborhood of  $k = 0$  is also sensitive to the accuracy of the integration.

In the present calculations, the phase function equa-

tion is integrated till  $\eta_1$  converges to the order of  $10^{-6}$ , which is consistent with the choice of tolerance. For Cs, this requires integration up to radial distances of  $\sim 500$ . The large radial distance is necessary as the phase shift is an asymptotic property. In addition, for the  $p$  wave scattering the centrifugal potential, which has  $R^{-2}$  dependence, vanishes at a slower rate compared to the van der Waals potential at large radial distances. This slows the convergences of the phase shift. A calculation of the  $s$  wave phase shift confirms this. The  $s$  wave phase shift  $\eta_0$  converges to the order of  $10^{-6}$  when the phase equation is integrated to a radial distance of  $\approx 100$ .

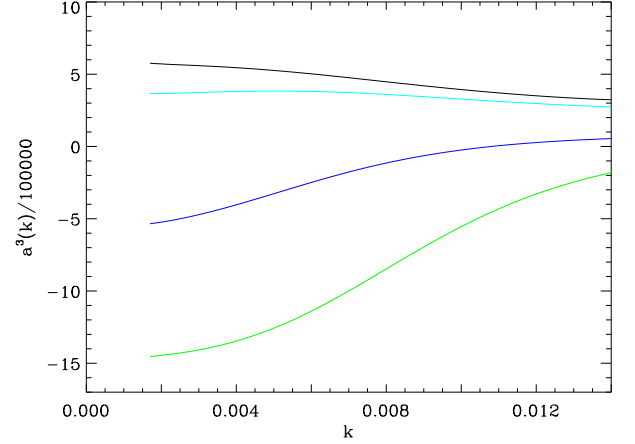


FIG. 5: Cube of scattering length  $a_1^3(k)$  or  $-\tan \eta_1/k^3$  for  $^{134}\text{Cs}$  is shown as a function of  $k$ . The black, green, blue and cyan correspond to  $R_c = 23.115, 23.165, 23.190$  and  $23.215$  respectively.

The values of  $-\tan(\eta_1(k))/k^3$  for  $^{134}\text{Cs}$  within a range of  $k$  for different  $R_c$  are shown in Fig.5. As discussed in ref. [12], the  $R_c = 23.165$  is a physically reasonable choice. For this the scattering length calculated as the slope of  $-\tan(\eta_1)/k^2$  in the  $k \rightarrow 0$  are 53 and -113 in atomic units for  $^{132}\text{Cs}$  and  $^{134}\text{Cs}$  respectively. This differs from the analytic values mentioned earlier by 61% and 4.4% for  $^{132}\text{Cs}$  and  $^{134}\text{Cs}$  respectively. It shows that the analytic expression though crude provides a good estimate for  $^{134}\text{Cs}$ , which has higher  $\gamma$ .

The evaluation of  $\eta_1$  from the numerically calculated  $A/B$  poses some difficulty. This is to do with the choice of appropriate  $R^*$ , the matching point, the dependence is shown in the Fig.6. The over all trend of the variation is rather complicated for the actual interatomic potential but less when only the van der Waals potential is considered. However, it is possible to calculate  $A/B$  from the value of  $a_1$  calculated earlier, which is obtained from the variable phase method. The value of  $A/B$  obtained from such a calculation are  $\approx -0.109$  and  $\approx 1.042$  for  $^{132}\text{Cs}$  and  $^{134}\text{Cs}$  respectively. The value of  $R^*$  around which  $A/B$  is close to this value occurs around the radial range of 23 – 24 atomic units. This is not surprising, as mentioned earlier, this is the radial range where the interatomic potential approaches the asymptotic form.

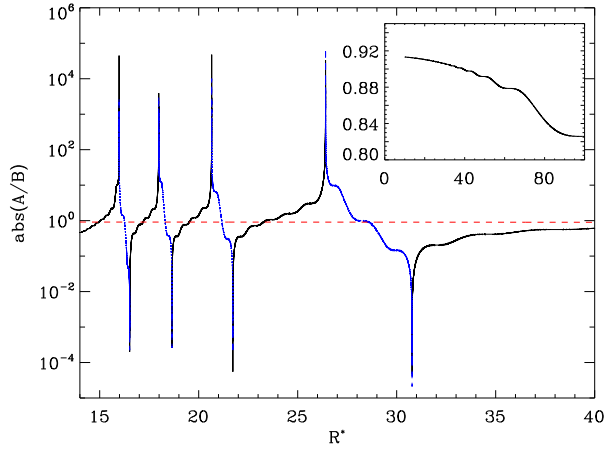


FIG. 6:  $|A/B|$  for  $^{134}\text{Cs}$  evaluated from the WKB solution is shown as a function of the matching point  $R^*$ . The black and blue portions of the curve indicate the positive and negative values of  $A/B$ . The dashed red curve shows the  $A/B$  when only the van der Waal's potential is considered and the inset plot shows the overall nature of the same.

## B. Lithium

For the  $a^3\Sigma_u^+$  state of  $^6\text{Li}_2$ , we use the interatomic potential suggested by Zemke and Stwalley [18]. The long range part of the interaction potential, for  $^7\text{Li}$  in particular, are discussed in ref. [14]. For the  $R \leq 6.388674$  and  $R \geq 18.0$  regions, the analytic expressions recommended in ref. [18] are used. Then, for the  $6.388674 < R < 18.0$  region, the interatomic potential is approximated as the cubic spline fitted to the potential values given by Zemke and Stwalley. A plot of the interatomic potential obtained is shown in Fig.7. As to be expected, the potential

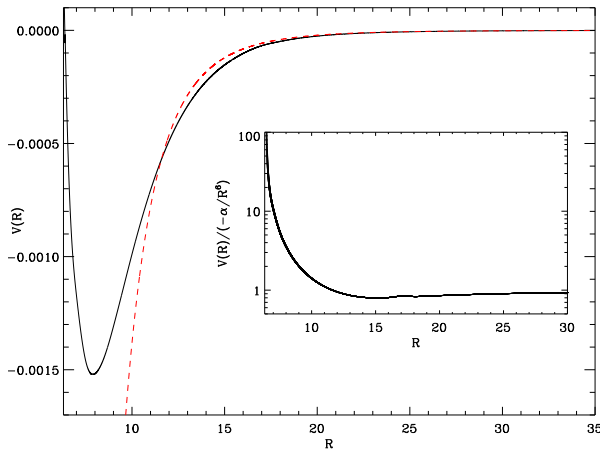


FIG. 7: Interatomic potential for  $a^3\Sigma_u^+$  of  $^6\text{Li}_2$ . The solid (black) and dash (red) are the interatomic potential and the van der Waal's potential respectively. The plot in the inset is the ratio of the van der Waal's potential and the interatomic potential.

approaches the asymptotic form, van der Waal's potential, at smaller radial distance compared to Cs. This is evident from a visual comparison of the two potentials shown in Fig.7 and Fig.3. This implies that, the phase shift calculation of lithium can have better convergence properties. Consequently, the methods adopted for the Cs calculations are applicable to Li and provide results with higher accuracy.

To optimize the calculations, we use the RKF method to solve Eq.(28) with relative tolerance varied as a function of  $k$ . The relative tolerance is set to  $10^{-5}$  for  $k > 0.01$  and it is lowered as  $k$  is decreased. This is essential as the scattering length depends on the nature of the phase shift in the neighborhood of  $k = 0$ . Based on extensive test calculations, the optimal choice of the relative tolerance is  $10^{-6}$  for  $0.01 \leq k < 0.005$  and  $10^{-7}$  for  $k \leq 0.005$ . With this choice it is possible to get reliable results for phase shift up to  $k = 0.0005$ . We find that phase shift stabilizes to 31.46 as  $k \rightarrow 0$  which is shown in Fig.8.

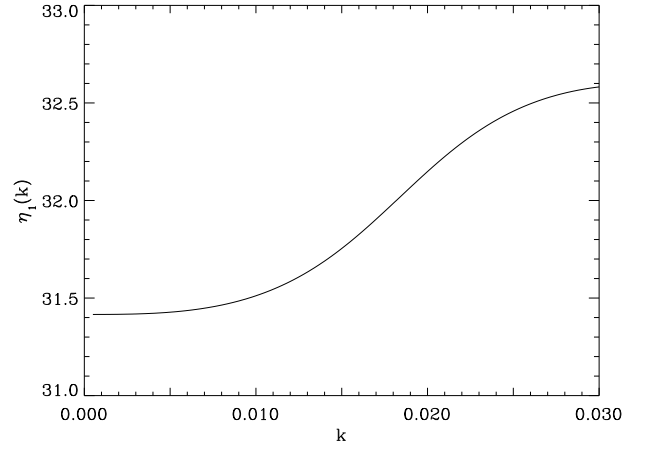


FIG. 8: The  $p$ -partial wave phase shift  $\eta_1(k)$  for the  $a^3\Sigma_u^+$  interaction potential of  $^6\text{Li}_2$ . The phase shift converges to 31.46 as  $k \rightarrow 0$ .

The sensitivity of the phase shift to the relative tolerance at low  $k$  is not very prominent from the values of  $\eta_1$ . However, it is not so with the  $-\tan(\eta_1)/k^3$ , which is the scattering length in the  $k \rightarrow 0$  limit. The small value of  $k$  and the transcendental function  $\tan$  enhances variations in  $\eta_1$ . This is evident when  $-\tan(\eta_1)/k^3$  as a function of  $k$  is compared at low  $k$  values for two different relative tolerances. The plot of such a comparison is shown as the inset plot in Fig.9. With improved tolerance, the lowest  $k$  value up to which the reliable phase shift can be calculated is decreased. There is however a limitation to decreasing the value of  $k$ , up to which the phase shift is calculated, by decreasing the value of relative tolerance. Below a certain value of relative tolerance, the RKF method fails to perform the integration of the phase equation up to the cut off point. From the calculations, we find that  $-\tan(\eta_1)/k^3$  stabilizes to  $\approx -92660$ , this is evident from the plot in Fig.9). The cube root of this is

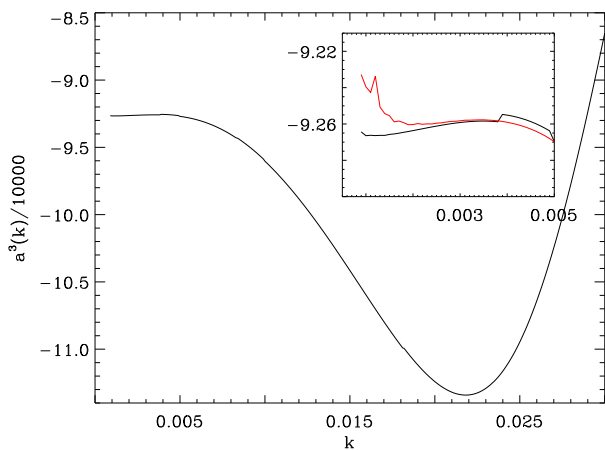


FIG. 9: Variation of  $-\tan(\eta_1)/k^3$  is plotted as a function of  $k$ . At low  $k$  values, the relative tolerance of the calculation is  $10^{-7}$ . The inset plot shows the sensitivity of  $-\tan(\eta_1)/k^3$  to the relative tolerance. The red and black curves in the inset correspond to tolerance of  $10^{-6}$  and  $10^{-7}$  respectively.

the  $a_1$ . Another equivalent way to calculate the scattering length is to evaluate the slope of  $-\tan(\eta_1)/k^2$  in the  $k \rightarrow 0$  limit. We calculate this by least square fitting the data points for  $-\tan(\eta_1)/k^2$  between  $0.0005 \leq k \leq 0.0005$  with an additional point corresponding to zero phase shift at  $k = 0$ . As is evident from Fig.(10) there is very good

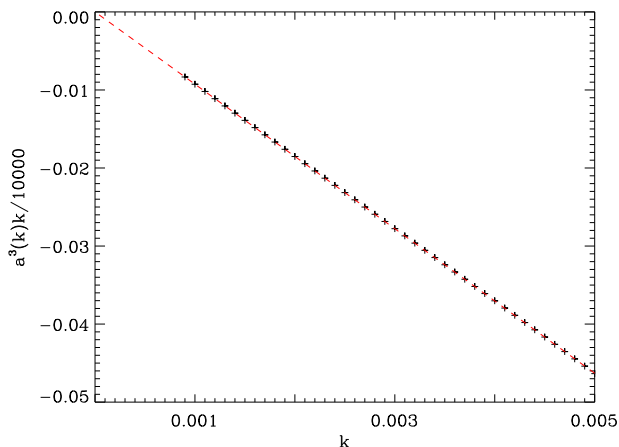


FIG. 10: Plot shows least square fitted line (dashed red curve) on  $a_1^3(k)k$  values in the domain  $0.0005 \leq k \leq 0.005$  (black crosses). An additional point coinciding with origin is also considered while drawing the least square fitted curve. The slope of this line is  $\approx -92600$ .

fitting of straight line over the data points. The slope of the least square fitted line is  $-92600$ , the cube root of which is  $-45$  and can be considered as a reliable value of the  $p$ -wave scattering length. If we compare it with the analytic approximation of  $a_1$  obtained by using Eq.(24) as the value of  $A/B$ , we find that percentage error incurred by using analytic approximation is 43.74 percent.

## VI. CONCLUSIONS

For  $p$  partial waves, the centrifugal term in the effective interatomic potential leads to a WKB solution, which is more complicated than the one without it as in  $s$  partial wave case. Consequently, the constant  $A/B$  of the partial wave solution evaluated has radial dependence and apriori, it is not possible to choose an appropriate  $R$  at which a reliable  $A/B$  can be evaluated. The approximate analytic expression to calculate  $A/B$  provide good results for  $^{134}\text{Cs}$  but has large errors for  $^{132}\text{Cs}$  and  $^6\text{Li}$ . Based on our calculations, using the variable phase method, we estimate the  $p$ -wave scattering length of  $^6\text{Li}$  is  $-45$ .

- 
- [1] B. DeMarco and D. S. Jin, Science **285**, 1703 (1999).
  - [2] H. T. Stoof, M. Houbiers, C. A. Sackett, and R. G. Hulet, Phys. Rev. Lett. **76**, 10 (1996); M. Houbiers, R. Ferwerda, H. T. C. Stoof, W. I. McAlexander, C. A. Sackett,

- and R. G. Hulet, Phys. Rev. A **56**, 4864 (1997).
- [3] J. Kinast, S. L. Hemmer, M. E. Gehm, A. Turlapov, and J. E. Thomas, Phys. Rev. Lett. **92**, 150402 (2004).
- [4] M. Bartenstein, A. Altmeyer, S. Riedl, S. Jochim1,



- C. Chin, J. H. Denschlag, and R. Grimm, Phys. Rev. Lett. **92**, 203201 (2004).
- [5] M. W. Zwierlein, J. R. Abo-Shaeer, A. Schirotzek, C. H. Schunck and W. Ketterle, Nature **435**, 1047 (2005).
- [6] M. M. Parish, F. M. Marchetti, A. Lamacraft and B. D. Simons, Nature Phys. **3**, 124 (2007).
- [7] Y. Shin, C. H. Schunck, A. Schirotzek and W. Ketterle, Nature **451**, 689 (2008).
- [8] M. Taglieber, A.-C. Voigt, T. Aoki, T. W. Hänsch, and K. Dieckmann, Phys. Rev. Lett. **100**, 010401 (2008).
- [9] M. M. Parish, F. M. Marchetti, A. Lamacraft, and B. D. Simons, Phys. Rev. Lett. **98**, 160402 (2007).
- [10] Z. Idziaszek and T. Calarco, Phys. Rev. Lett. **96**, 013201 (2006).
- [11] K. Kanjilal and D. Blume, Phys. Rev. A **70**, 042709 (2004).
- [12] G. F. Gribakin and V. V. Flambaum, Phys. Rev. A **48**, 546, (1993).
- [13] F. Calogero, *Variable phase approach to potential scattering* (Academic Press, New York, 1967).
- [14] R. Côté, A. Dalgarno and M. J. Jamieson, Phys. Rev. A **50**, 399 (1994).
- [15] N. F. Mott and H. S. W. Massey, *The theory of atomic collisions* (Oxford University Press, 1965).
- [16] H. Suno, B. D. Esry and C. H. Greene, Phys. Rev. Lett. **90**, 053202 (2003).
- [17] A. A. Radstig and B. M. Smirnov, *Parameters of Atoms and Atomic Ions Handbook*, (Energoatomizdat, Moscow, 1986).
- [18] W. T. Zemke and W. C. Stwalley, J. Phys. Chem. **97**, 2053-2058, (1993)
- [19] W. T. Zemke and W. C. Stwalley, J. Chem. Phys. **100**, 2661 (1994).
- [20] W. T. Zemke, C-C. Tsai and W. C. Stwalley, J. Chem. Phys. **101**, 10382 (1994).